Crystalline and amorphous phases of a new drug

**G. Bruni · C. Milanese · V. Berbenni ·
F. Sartor · M. Villa · A. Marini**

Abstract The thermodynamic properties of a new anti-depressant drug are studied from room temperature to 200 °C. In this range, the sample neither decompose, nor has a significant reactivity with water. When slowly heating a "fresh" sample, we may observe the following phenomena (in the order): melting of a form (F1, $\sim$170 °C), crystallization of a structurally different form (F2), and melting of F2 ($\sim$180 °C). In no circumstances, the direct transition from F1 to F2 can be observed. On the other hand, F2 reverts to F1 upon cooling below $\sim$130 °C. A glassy phase is formed upon cooling from above 180 °C, as confirmed by X-ray analysis and the appearance of a glass transition when reheating. The "reversible" (e.g., melting) and "irreversible" (e.g., glass formation) contributions to the measured enthalpies are estimated with temperature-modulated DSC measurements, resulting into a consistent description of thermodynamics of the forms, their melting and their kinetics of transformation.

Keywords Double melting · DSC · Enantiotropy ·
Polymorphism · TMDSC

G. Bruni (✉) · C. Milanese · V. Berbenni · A. Marini
Dipartimento di Chimica Fisica dell'Università degli Studi di
Pavia, C.S.G.I, Via Taramelli 16, 27100 Pavia, Italy
e-mail: giovanna.bruni@unipv.it

F. Sartor
Medicine Research Center, GlaxoSmithKline S.p.A, Via A.
Fleming 2, 37135 Verona, Italy

M. Villa
Dipartimento di Progettazione e Tecnologie, Università di
Bergamo, Bergamo, Italy

Introduction

GlaxoSmithKline has developed a new drug, code named GW597599B, successful in the treatment of unipolar depression. Its structure formula is:
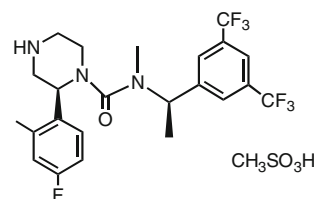
GW597599B is produced in the form of a white crystalline powder, which is soluble in water (with a pH dependent solubility) and in many organic solvents. Our previous studies on solid state drugs synthesized by GSK have shown the existence of complex phenomena of polymorphism [1], hydration [1] amorphisation [2], and decomposition [3], which all have a bearing in the pre-formulation problem.

A full characterization of a drug in the solid state is an essential step to achieve a target (or sufficient) stability and an optimal yield of its most useful form. This is particularly true in the presence of polymorphism [4–9], to which unexpected phase changes during the various stages of drug processing and scale-up are often associated. Frequently, a stable form is not available, or we have a form that does not achieve minimal targets, such as a solubility threshold, or that it is likely to switch to a nearly insoluble compound in the life span of the drug. In these cases, we need to identify the most stable form and the treatments that lead to it, or the conditions which delay an unwanted transformation, particularly during prolonged storage.

The traditional techniques for investigation of polymorphism are powder X-ray diffraction, differential scanning calorimetry, and thermogravimetric analysis [10, 11]. Useful information can be also obtained by temperature-modulated DSC (TMDSC), which is well-suited to clarify the nature of the thermal events associated with transformations between forms or phases [12–14]. DSC and TMDSC are crucial when we have polymorphs with melting temperatures that are very close. In our case, we will show that a solid form is created when the other one is melting. Of course, our main conclusions will be supported also by X-ray diffraction and scanning electron microscopy data, but DSC and TMDSC offer a unique insight about a complex thermal phenomenon and its reversing and non-reversing contributions.

We will focus our attention into the region below 200 °C, where preliminary measurements with a variety of techniques (thermal analysis, X-ray diffraction, SEM, and FT-IR) in different conditions (sealed/open pans, wet/dry atmosphere) have shown that the thermal phenomena are not affected by exchanges with a gaseous phase. In particular, below 200 °C, there are no significant hydration/dehydration processes and no decomposition apparently occurs. This fact greatly simplifies the analysis of the thermal response and permits to accurately identify the parameters of the different forms and the nature (reversible/irreversible) of the transformation among them and the liquid state.

Experimental

The experiments have been performed with samples from two different production batches, which were stored at 4 °C in sealed containers and used as received from Glaxo-SmithKline. All data reported here refer to samples from a single batch, but we did not find significant differences in the thermal response of samples from the second batch.

A set of simultaneous TG/DSC runs have been made under different conditions (in wet or dry nitrogen, or in sealed containers) to ascertain the hydration/dehydration behavior and the presence of decomposition. Concerning hydration, we noted that samples as received and in dry atmosphere do not show any significant mass loss up to the temperature region of decomposition, which is above 200 °C. Here, we discuss only experiments performed in dry nitrogen, or sealed containers, with dry (as received) samples. No important differences are noted between measurements performed with sealed containers and open containers in dry N_2. Some samples were subjected to more than one thermal scan, but were never exposed to temperature higher than 190 °C before the last heating.

The thermal data have been acquired with the following systems:

– simultaneous DSC/TG analyser, mod. STA 625 by Polymer Laboratories (UK);
– heat flux calorimeter with temperature modulation (TMDSC), mod. TA 2920 by TA Instruments (USA), interfaced with an acquisition system (TA 5000); temperature modulation was achieved by an automatic liquid nitrogen accessory (LNCA by TA).

Microscopic images have been obtained with a Cambridge (UK) Stereoscan 200 Scanning Electron Microscope; diffraction patterns have been acquired with a Bruker (Bruker–Siemens, Germany) D 5005 powder X-ray diffraction system (Cu Kα radiation), equipped with a temperature chamber (TTK 450) and a graphite bent monochromator.

Results and discussion

Thermal effects: qualitative and quantitative aspects

Figure 1 compares two DSC runs performed at different heating rates (β): when β is 10 °C/min, two well-resolved endothermic peaks are observed (Fig. 1a); when β = 50 °C/min (Fig. 1b) only a single peak can be seen. In Fig. 1b, we identify
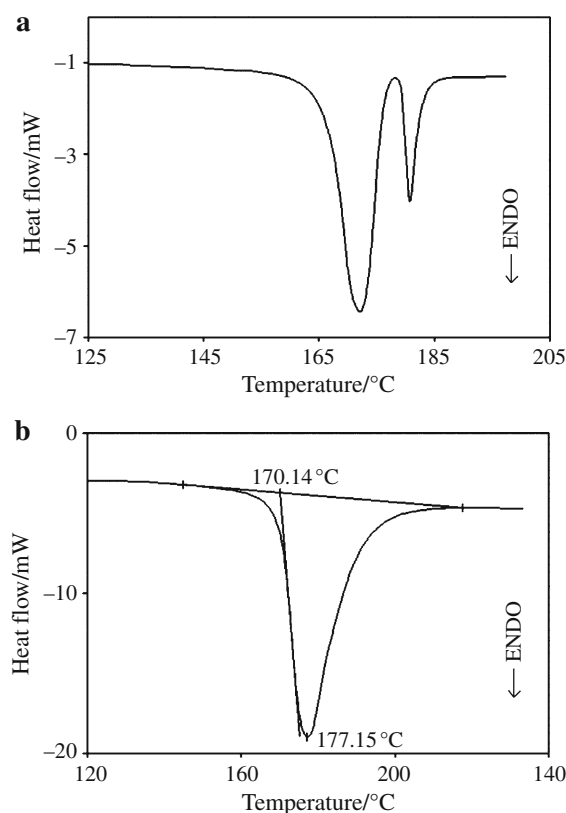

Fig. 1 DSC scans in dry nitrogen and sealed aluminum pans performed at 10 °C/min (**a**) and 50 °C/min (**b**). In **b**, the onset temperature and peak baseline are identified

the onset temperature ($T_{onset,1} = 170.14$ °C), the peak temperature ($T_{peak,1} = 177.15$ °C), the baseline, and the boundaries needed to compute the peak enthalpy ($\Delta H_{exp,1}$). When the second peak is present, the corresponding quantities will be indicated by $T_{onset,2}$, $T_{peak,2}$, and $\Delta H_{exp,2}$.

By decreasing the heating rate below 10 °C/min, an exothermic displacement occurs between the two endothermic phenomena, which eventually taken the form of a well-defined peak (see Fig. 2). For $\beta \leq 5$ °C/min, we may assign a characteristic temperature T_{exo} and an enthalpy $\Delta H_{exp,exo}$ to this peak. The thermal behavior of the sample as a function of the heating rate is summarized in Table 1, where we report the temperatures and enthalpies are defined above.

We call attention to the fact that $|\Delta H_{exp,1}|$ decreases with decreasing β, while both $|\Delta H_{exp,2}|$ and $|\Delta H_{exp,exo}|$ have an opposite behavior with β. The overall enthalpy change,

$$\Delta H_{exp,tot} = \Delta H_{exp,1} + \Delta H_{exp,2} + \Delta H_{exp,exo}$$

stay about the same when β is changed by two orders of magnitude; its average value is 55.8 J/g with a standard deviation <2% (~ 0.9 J/g).
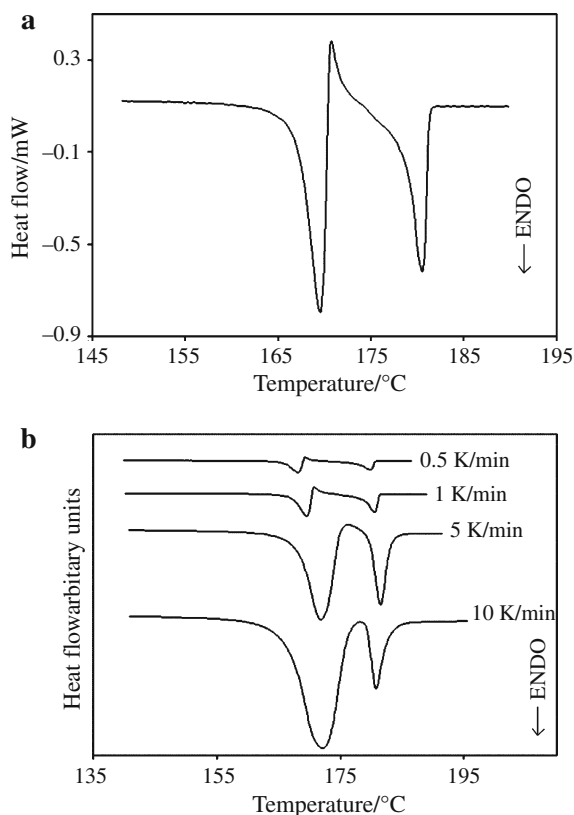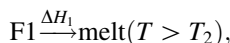

Fig. 2 DSC scan at 1 °C/min (**a**, *top*) and collection of scans at rates ≤10 °C/min (**b**, *bottom*), acquired in dry nitrogen and sealed aluminum pans

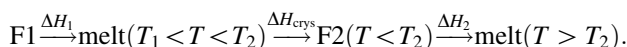## The nature of thermal effects

A qualitative interpretation of these observations is as follows. There are two forms of GW597599B: the one which is stable at room temperature (form F1) begins melting near 170 °C, whereas a second one is in solid phase (form F2) becomes thermodynamically stable. Crystallization of F2 is a relatively slow kinetic process which does not occur appreciably at high scanning rates. At low β, F2 is formed, which melts near 180 °C. The existence of a high temperature solid form (F2) different from that of room temperature (F1) is demonstrated by XRPD measurements. The patterns shown in Fig. 3 have been collected on the same sample at room temperature (a) and at 172 °C (b) where it is apparent that a new solid form is present.

Apparent enthalpies and melting enthalpies

It is quite natural to assume that a single liquid phase exists (produced by melting of either F1 or F2), and that the enthalpy of crystallization of F2 (ΔH_{crys}) has the same absolute value as the enthalpy of melting of this phase ΔH_2. Therefore, we achieve a molten phase either directly from F1, with enthalpy ΔH_1, or by going through F2:

$$F1 \xrightarrow{\Delta H_1} melt(T > T_2),$$

or

$$F1 \xrightarrow{\Delta H_1} melt(T_1 < T < T_2) \xrightarrow{\Delta H_{crys}} F2(T < T_2) \xrightarrow{\Delta H_2} melt(T > T_2).$$

Here, with T_1 and T_2, we indicate the true melting temperatures of the two forms. The experimentally deduced enthalpies are, to various degrees, a superposition of the three processes (two of melting, one of crystallization). However, at the highest rate, formation of F2 should be negligible, and we may identify $\Delta H_{exp,1}$ (~ 55.6 J/g) with the melting enthalpy of F1, ΔH_1. At the slowest rate, F2 is fully formed, and we can assume that $\Delta H_{exp,2} \approx \Delta H_2 = 27$ J/g.

In general, the experimental enthalpies may be written in terms of the melting enthalpies and the fractional masses, m_1 and m_c, which crystallize during the endothermic process (peak 1) and the exothermic one (peak "exo"), respectively:

$$\Delta H_{exp,1} = \Delta H_1 - m_1 \cdot \Delta H_2$$
$$\Delta H_{exp,exo} = -m_c \cdot \Delta H_2$$
$$\Delta H_{exp,2} = (m_1 + m_c) \cdot \Delta H_2$$
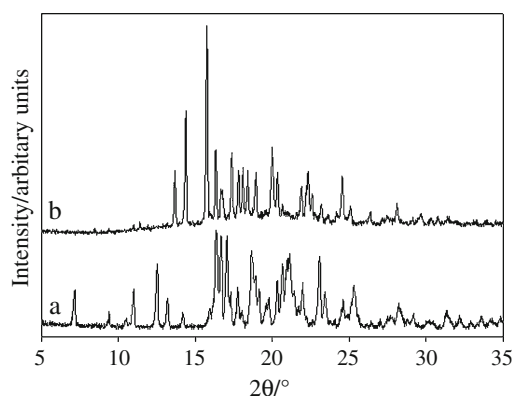$$\Delta H_{exp,1} + \Delta H_{exp,exo} + \Delta H_{exp,2} = \Delta H_1.$$

Thus, it is expected that the total enthalpy change is independent on β and coincides with the melting enthalpy of F1. This is exactly what happens the enthalpy change

Table 1 Experimental specific enthalpies and temperatures of melting (peaks 1, 2) and crystallization (peak "exo") for different heating rates

β/°C/min	$T_{onset,1}$/°C	$T_{peak,1}$/°C	T_{exo}/°C	$T_{onset,2}$/°C	$T_{peak,2}$/°C	$\Delta H_{exp,1}$/J/g	$\Delta H_{exp,exo}$/J/g	$\Delta H_{exp,2}$/J/g	$\Delta H_{exp,tot}$/J/g
50	172.0	179.0	–	–	–	55.6	–	–	55.6
40	171.0	177.7	–	–	–	56.8	–	–	56.8
30	170.0	176.2	–	ND	ND	ND	–	ND	55.9
20	169.1	174.8	–	ND	182.3	ND	–	ND	54.2
10	167.2	172.3	–	179.7	181.3	47.1	–	9.2	56.3
5	168.2	171.9	176.1	179.8	181.5	42.1	−2.5	16.5	56.2
1	165.1	168.2	169.3	176.8	178.9	36.5	−5.6	25.8	56.7
0.5	164.8	167.3	168.5	176.7	179.1	31.7	−3.7	27.0	55.0

Each datum is the average of those obtained in at least three different runs (standard deviations of the enthalpy data lower than 3%)

ND = not determined. ND is used when a peak, although present, is not sufficiently well resolved

Fig. 3 XRPD patterns recorded at 27 °C (**a**, *bottom*) and 172 °C (**b**, *top*)

Fig. 4 Plot of the overall F2 mass fraction which crystallizes (and then melts) as a function of the time spent between the melting temperatures of F1 and F2. Solid line is the fit to an exponential process

obtained at 50 °C/min, when the only thermal process is the melting of F1, is identical, within experimental error, to the total enthalpy change obtained at slower heating rates, where different thermal contributions are simultaneously present.
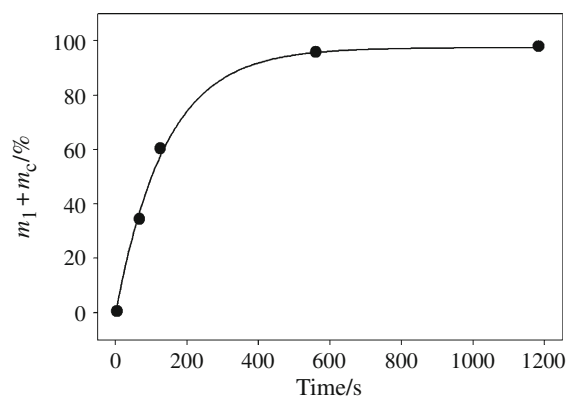
Figure 4 shows the behavior of $m_1 + m_c$ as a function of the time t spent in going from T_1 to T_2, which have been tentatively identified with 170 and 180 °C, respectively. The data points are fitted reasonably well by the equation

$$m_1 + m_c = 1 - \exp(-Wt)$$

with a rate $W \sim 1/160$ s.

Reversibility and double annealing experiments

The question naturally arises as to whether a transition between F1 and F2 solid forms may be observed or not. The answer is negative for the F1 → F2 transition. We never found evidence of a reduced $\Delta H_{exp,tot}$ (expected if F2 had formed) even in samples that have been annealed for hours slightly below T_1. In subsequent heating, melting, and crystallization resumed, as if no annealing had occurred.

On the other hand, evidence for a F2 → F1 transition upon cooling is obtained through "double annealing experiments." The idea is to bring the sample to a temperature ($T_{ann,1}$) above T_1 and below T_2 (i.e., at T slightly higher than 170 °C), and let it there long enough (~15 min) to allow complete conversion to F2. Then, the sample is cooled (at 1 °C/min) to a lower temperature ($T_{ann,2} < T_1$), where it is kept 15 min before being heated (again at 1 °C/min) across to the melting region. The most interesting run is obtained when $T_{ann,2} \approx 145$ °C: no major thermal effect is seen during cooling to $T_{ann,2}$, and during the second heating, only a single endothermic peak is observed with $T_{onset} = 176.1$ °C and enthalpy change $\Delta H \sim 30$ J/g. The T_{onset} value suggests that F2 is present in a consistent amount after the isothermal stage at $T_{ann,2} \approx 145$ °C. However, both the enthalpy value (higher than that assumed for pure F2 melting) and the peak shape (a long tail is present toward low temperature) indicate that a minor fraction of F1 is still present.

The behavior of samples treated with $80 \leq T_{ann,2} \leq 130$ °C is quite different:

1. upon cooling from $T_{ann,1}$, an exothermic peak occurs, which begins at a well-defined temperature (onset at 128.8 °C with a standard deviation of just 1.1 °C) and with a well-defined exothermic enthalpy, $\Delta H_{cool} = -23.1$ J/g (standard deviation <2%) computed only from the five experiments with $T_{ann,2} \leq 120$ °C, where peak areas can be reliably estimated;

2. upon the subsequent heating, an exothermic phenomenon, sandwiched between two endothermic peaks, occurs, with enthalpy values (standard deviations of about 3%) somewhat different from those of fresh samples scanned at the same heating rate: $\Delta H_{exp}(1) \approx 35.3$ J/g versus 36.5 J/g;

3. $\Delta H_{exp,exo} \approx 7.0$ J/g versus 5.6 J/g,

4. $\Delta H_{exp,2} \approx 20.7$ J/g versus 25.8 J/g.

The reproducibility of annealing experiments is quite remarkable. These data point to a limiting temperature around 140 °C as the lower boundary for the existence of F2, and to significant asymmetries (hysteresis) between heating and cooling. These asymmetries arise from a partial irreversibility of the processes, which will be further explored in the following. In particular, note that the value of the transition enthalpy that can be obtained by the melting enthalpies of the two pure solid forms:

$$\Delta H_1 - \Delta H_2 \approx (55.6 - 27.0)\text{J/g} = 28.6\,\text{J/g}$$

is $\sim 25\%$ higher than $|\Delta H_{cool}|(\approx 23.1$ J/g), which is also due to the enthalpy difference between F1 and F2.

Reversibility and double scan experiments

We have performed two subsequent heating runs above T_2 (i.e., to a fully melted sample), interleaved by a cooling (at the same rate of the heating) and by an annealing at 27 °C (for 15 min). When $\beta = 10$ °C/min, no exothermic solidification is observed upon cooling, and a characteristic glass transition phenomenon occurs near 75 °C upon the second heating. On the other hand, when β is 1 °C/min, we observe an exothermic shift during cooling. During heating, we have in the order: a small glass transition at 75 °C, a substantial and broad exothermic phenomenon beginning at 127 °C, the usual melting of F1, followed by crystallization of F2, and melting of F2, all above 170 °C. These phenomena indicate that irreversibility is related to formation of a glassy phase, which may be "frozen" when cooling rapidly. Otherwise, we have substantial recrystallization (into form F1, beginning around 128 °C) upon reheating when heating rate is relatively low (1 °C/min).

We call attention to the fundamental differences between the thermal responses of samples, which have been heated just above T_1 and those which went past T_2. During the subsequent heating, a glass transition occurs
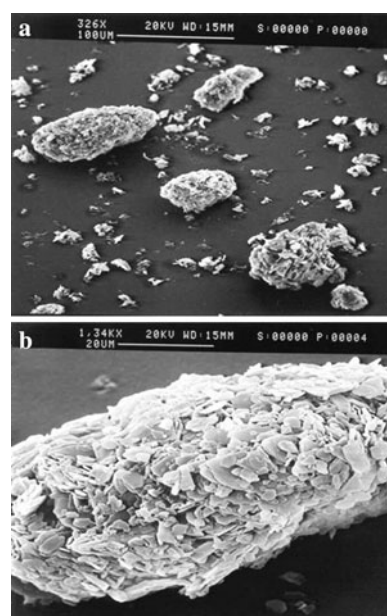

Fig. 5 SEM of an as-received sample

only with the latter ones, i.e., only samples which have been fully melted display a glass transition, while the other ones display only a solid-to-solid transition upon cooling.

The picture deduced from thermal measurements is confirmed by SEM and XRPD experiments. Micrographs of an as-received sample are shown in Fig. 5. A sample heated up to 190 °C (than fully melted) and cooled to room temperature at 10 °C/min is shown in Fig. 6: it is apparent that morphology is dramatically changed, and that the sample is now constituted by blocks of glassy aspect. The micrographs of Fig. 7 refer to a glassy sample slowly heated (1 °C/min) up to 130 °C and maintained at this temperature for 1 h. A comparison with Fig. 6 makes it clear that the consequence of the annealing at 130 °C is the crystallization of the glassy phase. The X-ray patterns of the samples which underwent the same treatments as the samples of Figs. 5, 6, and 7 are shown in Fig. 8. It appears that: (a) the fully melted sample does not show any reflection, (b) the annealed sample is a crystalline one, and (c) a sample as received gives the same reflections as the sample annealed at 130 °C.

TMDSC measurements

Further insights into the role of reversing (melting) and non-reversing (glass forming) processes in GW597599B have been obtained by temperature-modulated DSC experiments. The relevant results are summarized in Table 2. The first three experiments have been performed with different modulation periods (P from 50 to 80 s), and by choosing the modulation amplitude (A/°C) in such a way that the instantaneous heating rate varied from $\beta_{min} = 0$ °C/min to
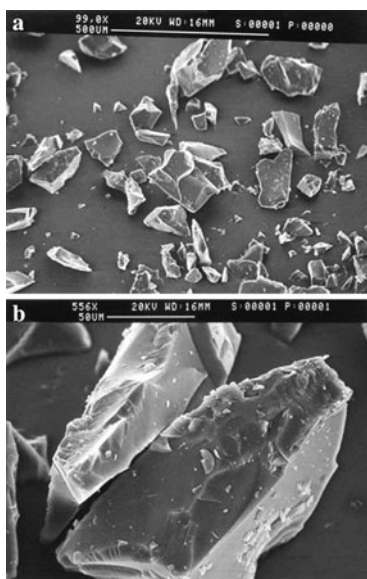
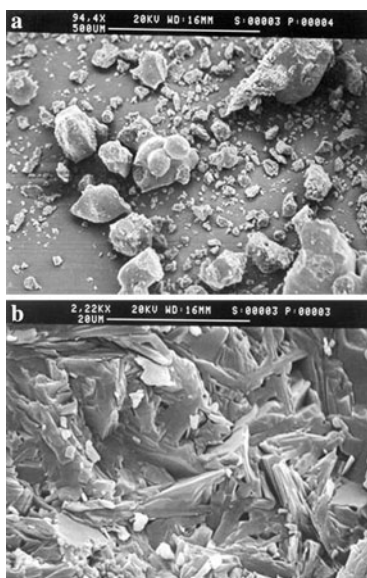**Fig. 6** SEM of a sample melted (at 190 °C) and solidified into a glass

Fig. 7 SEM of a glassy sample after annealing at 130 °C

$\beta_{\max} = 2$ °C/min. When the period is increased by 60% (from 50 to 80 s), we note that a decrease by nearly the same amount of the non-reversing contribution to peak 2, and a similar increase of the reversing contribution. The changes of the contributions to peak 1 are in the same direction, but substantially smaller (about 20%). A stable melting process, such as that of F2, is thermodynamically reversible. However, due to the dynamic conditions of a DSC measurement, the process is far from thermodynamic equilibrium and may show a kinetic or non-reversing component. Equilibrium conditions are better approached by increasing the period and, as expected, the reversing component of F2 melting
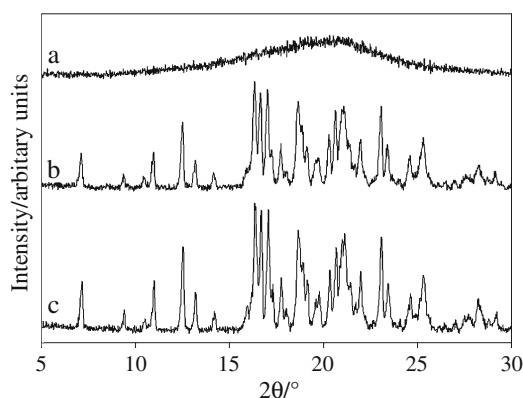

Fig. 8 Diffraction patterns of: (**a**) sample cooled to room temperature from 190 °C at 10 °C/ min (glassy sample); **b** the same sample after annealing at 130 °C for 1 h; **c** as-received sample. All these patterns have been collected in dry N_2 atmosphere

greatly increases with increasing the period. The fact that such a behavior is much less evident for the melting of F1 suggests that this process has intrinsic elements of non-reversibility, or that, due to its own kinetics, a period increase is scarcely effective.

The last three lines in Table 2 refer to experiments performed at constant period and different average heating rate and/or modulation amplitudes. Note that an increase of the modulation amplitude at an average rate $\beta = 1$ °C/min (compare lines two and five of the table) does not change appreciably the contributions (reversing and non-reversing) to peaks 1 and 2.

In the fifth line of Table 2, the underlying heating rate was increased at $\beta = 3$ °C/min and the amplitude selected to return to a minimum heating rate of 0 °C/min, and to have a maximum heating rate of 6 °C/min. The most homogeneous comparison is again with the data of the second line of the Table. As it can be seen, the reversing components of both melting peaks consistently increase: for the first time, the reversing component of peak 1 becomes prevalent on the non-reversing one, while the reversing component of peak 2 accounts for over 90% of the melting enthalpy of F2. However, note that while the increase of the reversing component of peak 1 is both relative and absolute, that of peak 2 is mainly relative. In other words, the total melting enthalpy of peak 2 is decreased at the expenses of the non-reversing component, which is now very small. In contrast, the total melting enthalpy of peak 1 is increased. We know, after discussion of conventional DSC measurements, that the expected effect of an increase of the underlying heating rate is just an increase of the melting enthalpy of peak 1 and a decrease of that of peak 2. The relative increase of the reversing components of both peaks is also expected. On the other hand, an amplitude increase at $\beta = 3$ °C/min

Table 2 Summary of the MTDSC runs with a given period (*P*), amplitude (*A*), average rate (*β*), and minimum and maximum rate

P/s	*A*/°C	*β*/°C/min	*β*$_{min}$/°C/min	*β*$_{max}$/°C/min	$\Delta H_{exp,1}$/J/g		$\Delta H_{exp,2}$/J/g	
					REV	NREV	REV	NREV
50	0.133	1	0	2	8.7	23.3	11.0	15.1
60	0.159	1	0	2	12.7	19.9	14.9	10.9
80	0.212	1	0	2	13.0	17.8	18.5	6.6
60	0.318	1	−1	3	13.4	18.9	13.7	10.7
60	0.477	3	0	6	23.7	14.0	16.2	1.4
60	0.716	3	−1.5	7.5	12.8	19.4	13.2	3.2

Deconvolution of the enthalpies for peaks 1 and 2 into a reversible (REV) and an irreversible (NREV) contribution is given

causes an important increase of the non-reversing components, particularly that of peak 2.

Conclusions

GW597599B displays a relatively simple double melting behavior. A similar behavior could be shown both by an enantiotropic compound (due to a slow kinetic of the solid state transition from the low temperature to the high temperature form) and by a monotropic compound (due to the melting of the metastable solid form before formation of the stable form). Glass formation and re-crystallization upon reheating account for thermal hysteresis. Some light upon the phenomenon is shed by application of the thermodynamic model of Yu [6] to our data. Adapting his equations to our case, we may obtain the following theoretical expression for the transition temperature T_t:

$$T_t = \frac{[\Delta H_1 - \Delta H_2 + 0.003 \cdot \Delta H_2 \cdot (T_2 - T_1)]}{\frac{\Delta H_1}{T_1} - \frac{\Delta H_2}{T_2} + 0.003 \cdot \Delta H_2 \cdot \ln \frac{T_2}{T_1}}$$

where 0.003 is a coefficient which applies a small empirical correction arising from the difference in heat capacity between liquid and F2.

We obtain a transition temperature of 165 °C, which is: (a) lower than the lowest value obtained for $T_{onset,2}$ (176.7 °C, see Table 1); (b) identical, within experimental error, to the lowest value of $T_{onset,1}$ (164.8 °C, see Table 1).

Point (a) indicates that F1 and F2 are in enantiotropic relationship, that is each one has its own temperature range of thermodynamic stability (T_t should be higher that $T_{onset,2}$ if the two forms were in monotropic relationship). The fact that $\Delta H_1 > \Delta H_2$ confirms such a conclusion: if the two forms were in monotropic relationship, we should have found exactly the opposite [12]. Point (b) explains why F2 cannot be directly obtained from F1: at $T_{onset,1}$, the endothermic deviation of the DSC curve has already begun, so that the solid state transition temperature occurs after a "pre-melting" of F1 has already started. In contrast, it is possible to prepare a supercooled F2 phase and readily observe the F2 → F1 transition down to 80 °C.

References

1. Marini A, Berbenni V, Bruni G, Margheritis C, Orlandi A. Physico-chemical study of the solid forms of a new drug. J Pharm Sci. 2001;90:2131–40.
2. Marini A, Berbenni V, Bruni G, Sinistri C, Maggioni A, Orlandi A, et al. Physico-chemical characterization of a novel tryciclic β-lactam antibiotic. J Pharm Sci. 2000;89:232–40.
3. Marini A, Berbenni V, Bruni G, Villa M, Orlandi A. Thermal decomposition and melting of a new caboxyindole derivative. J Therm Anal Calorim. 2002;68:389–96.
4. Haleblian J, McCrone W. Pharmaceutical applications of polymorphism. J Pharm Sci. 1969;58:911–29.
5. Vippagunta SR, Brittain HG, Grant DJW. Crystalline solids. Adv Drug Deliv Rev. 2001;48:3–26.
6. Yu L. Inferring thermodynamic stability relationship of polymorphs from melting data. J Pharm Sci. 1995;84:966–74.
7. Hilfiker R. Polymorphism in the pharmaceutical industry (Chap. 1, 2). Weinheim: Wiley-VCH; 2006.
8. Lee EA, Sohn YT. Crystal forms of a capsaicin derivative analgesic DA-5018. J Therm Anal Calorim. 2008;93:871–4.
9. Drebushchak VA, Drebushchak TN, Chukanov NV, Boldyreva EV. Transitions among five polymorphs of chlorpropamide near the melting point. J Therm Anal Calorim. 2008;93:343–51.
10. Giron D. Thermal analysis and calorimetric methods in the characterisation of polymorphs and solvates. Thermochim Acta. 1995;248:1–59.
11. Rodriguez-Spong B, Price CP, Jayasankar A, Matzger AJ, Rodrıguez-Hornedo N. General principles of pharmaceutical polymorphism: a supramolecular perspective. Adv Drug Deliv Rev. 2004;56:241–74.
12. Coleman NJ, Craig DQM. Modulated temperature differential scanning calorimetry: a novel approach to pharmaceutical thermal analysis. Int J Pharm. 1996;135:13–29.
13. Gill PS, Sauerbrunn SR, Reading M. Modulated differential scanning calorimetry. J Therm Anal Calorim. 1993;40:931–9.
14. Burger A, Ramberger R. On the polymorphism of pharmaceutical and other crystals, I: theory of thermodynamic rules. Microchim Acta II. 1979;72:259–71.